NIH Public Access
Author Manuscript
*Mol Pharm*. Author manuscript; available in PMC 2011 August 1.

Published in final edited form as:
*Mol Pharm*. 2010 August 2; 7(4): 1209–1222. doi:10.1021/mp100043h.

# Cytochrome c Encapsulating Theranostic Nanoparticles: A Novel Bifunctional System for targeted delivery of therapeutic membrane-impermeable proteins to tumors and imaging of cancer therapy

**Santimukul Santra**[‡], **Charalambos Kaittanis**[‡,#], and **J. Manuel Perez**[‡,#,*]

[‡]Nanoscience Technology Center, University of Central Florida, 12424 Research Parkway, Suite 400, Orlando, FL 32826

[#]Burnett School of Biomedical Sciences – College of Medicine, University of Central Florida, 12424 Research Parkway, Suite 400, Orlando, FL 32826

[*]Department of Chemistry, University of Central Florida, 12424 Research Parkway, Suite 400, Orlando, FL 32826

## Abstract

The effective administration of therapeutic proteins has received increased attention for the treatment of various diseases. Encapsulation of these proteins in various matrices, as a method of protein structure and function preservation, is a widely used approach that results in maintenance of the protein's function. However, targeted delivery and tracking of encapsulated therapeutic proteins to the affected cells is still a challenge. In an effort to advance the targeted delivery of a functional apoptosis-initiating protein (Cytochrome c) to cancer cells, we formulated theranostic polymeric nanoparticles for the simultaneous encapsulation of Cytochrome c and a near infrared dye to folate-expressing cancer cell cells. The polymeric nanoparticles were prepared using a novel water soluble hyperbranched polyhydroxyl polymer that allows for dual encapsulation of a hydrophilic protein and an amphiphilic fluorescent dye. Our protein therapeutic cargo is the endogenous protein Cytochrome c, which upon cytoplasmic release, initiates an apoptotic response leading to programmed cell death. Results indicate that encapsulation of Cytochrome c within the nanoparticle's cavities preserved the protein's enzymatic activity. The potential therapeutic property of these nanoparticles was demonstrated by the induction of apoptosis upon intracellular delivery. Furthermore, targeted delivery of Cytochrome c to folate-receptor-positive cancer cells was achieved via conjugation of folic acid to the nanoparticle's surface, whereas the nanoparticle's theranostic properties were conferred via the co-encapsulation of Cytochrome c and a fluorescent dye. Considering that these theranostic nanoparticles can carry an endogenous cellular apoptotic initiator (Cytochrome c) and a fluorescent tag (ICG) commonly used in the clinic, their use and potential translation into the clinic is anticipated, facilitating the monitoring of tumor regression.

### Keywords

hyperbranched polymer; polymeric nanoparticles; biodegradable; Cytochrome c; encapsulation; peroxidase activity; cytotoxicity; internalization; targeted delivery; optical imaging; cancer therapy

[*]Corresponding Author: Nanoscience Technology Center, University of Central Florida. 12424 Research Parkway, Suite 400, Orlando, FL 32826. Ph: 407-882-2843. Fax: 407-882-2819. jmperez@mail.ucf.edu.

NIH-PA Author Manuscript
NIH-PA Author Manuscript
NIH-PA Author Manuscript

NIH-PA Author Manuscript

NIH-PA Author Manuscript

NIH-PA Author Manuscript

## Introduction

The targeted delivery of therapeutic proteins, genes and other biomacromolecules to specific locations within the body could have a tremendous impact in the treatment of various conditions such as cancer, cardiovascular and infectious diseases.1 To achieve this goal, these biomacromolecules are typically encapsulated in polymeric matrices to improve their stability in serum, delivery, and therapeutic efficacy.2, 3 Protein delivery is of particular importance, because a signaling protein can be encapsulated and specifically delivered to cancer cells to trigger a specific physiological response such as apoptosis.4 The intracellular delivery of membrane-impermeable proteins is an emerging research topic for therapeutic applications. Recently, silica nanoparticles and carbon nanotubes have been used as effective delivery nanosystems for the delivery of proteins and DNA into the cell.4–6

Cytochrome c (Cyt C) is a small mitochondrial protein (MW= 12 KDa) that plays a key role in cellular respiration. The enzyme, although highly water soluble, when present in the mitochondrial inter-membrane space is loosely bound to the inner membrane where it facilitates electron transport between Cytochrome c reductase (complex III) and cytochrome oxidase (complex IV), within the mitochondria's electron transport chain.7 In addition, Cyt C has also been identified as an important mediator of apoptosis, a normal process of controlled cell death that is important during development and upon substantial and irreparable cell damage.4, 7–9 Under these conditions, the apoptotic cascade is initiated, leading to activation of downstream apoptotic effectors, such as Bax, a member of the Bcl-2 protein family.10, 11 Translocation of Bax from the cytoplasm to the outer mitochondrial membrane results in the initial dimerization and oligomerization of Bax on the mitochondrial membrane, facilitating the formation of a permeability transition pore and therefore achieving the release of Cyt C from the mitochondria to the cytoplasm.10, 11 Once in the cytoplasm, Cyt C initiates a molecular cascade that results in proteolytic cleavage on a wide range of cellular proteins, as part of the programmed cell death repertoire.7, 8 However, in some cases cancer cells develop ways to evade the release of mitochondrial Cyt C into the cytoplasm even in the presence of extensive DNA abnormalities, by preventing the activation and recruitment of proapoptotic Bcl-2 family members to the outer membrane and therefore abrogating the formation of the mitochondrial permeability transition pore.12 These cells continue dividing, even in the presence of extensive DNA damage, leading to tumorigenesis.

Therefore, it would be ideal to develop cancer therapeutics for the targeted induction of apoptosis in cancer cells. For instance, the targeted delivery of Cyt C to cancer cells could selectively initiate apoptosis in these cells, while not affecting healthy cells, making this approach an attractive cancer therapeutic strategy.13 To this goal, we have synthesized a novel biocompatible and targetable polymeric nanoparticle capable of encapsulating both Cyt C and fluorescent dyes for targeted cancer therapy and optical imaging. The polymeric nanoparticles are made from a novel water-soluble hyperbranched polyhydroxyl (HBPH) polymer that upon dispersion in aqueous media it self assemble such that most of the hydroxyl groups are exposed to the aqueous environment. This process allows the formation of highly stable and monodisperse nanoparticles with amphiphilic nanocavities that facilitate the encapsulation a hydrophilic protein such as Cyt C. In addition, due to the amphiphilic nature of the nanocavity, amphiphilic fluorescent dyes (e.g., DiI and ICG) can be encapsulated into the nanoparticle without compromising encapsulation of the hydrophilic protein.

The HBPH nanoparticle was designed to encapsulate hydrophilic cargos (such as proteins) inside its amphiphilic nanocavities. We hypothesized that during nanoparticle formation a

NIH-PA Author Manuscript

NIH-PA Author Manuscript

NIH-PA Author Manuscript

stable encapsulation of Cyt C will take place inside the polymeric nanocavities due to the presence at physiological pH of positively charged lysine residues on the protein's surface that can interact electrostatically with the electronic environment within the HBPH nanocavities (Scheme 1). The presence of several electronegative atoms in the polymer structure (e.g., oxygen and nitrogen) with lone pairs of electrons makes the polymeric nanocavities partially negative in nature. In addition, the presence of multiple esters, tertiary amines and alcohol groups within the nanocavities can form multiple hydrogen bonds with Cyt C lysine residues, further stabilizing the encapsulation. This contrasts with our previously reported hydrophobic hyperbranched polyester (HBPE) polymer14 that when dispersed in aqueous media forms nanoparticles with hydophobic nanocavities that can only encapsulate hydrophobic cargos.

Results showed that upon HBPH encapsulation, Cyt C did not suffer any loss-of-function as the catalytic (peroxidase) activity of both the encapsulated and released Cyt C was equivalent to that of the non encapsulated protein. Furthermore, we discovered that the Cyt C-HBPH were selectively uptaken by various human carcinoma cells resulting in apoptosis (programmed cell death), after Cyt C's release into the cytoplasm. Our results indicate the targeted delivery, monitoring and treatment capabilities of our Cyt C-encapsulating HBPH theranostic nanoparticles.

## Experimental Section

### Materials

Anhydrous DMF, DMSO, Indocyanine green (ICG), Cytochrome c (from horse heart), 3-(4,5-Dimethylthiazol-2-yl)-2,5-diphenyltetrazolium bromide (MTT), 1,1'-Carbonyldiimidazole (CDI), *N*-hydroxysuccinimide (NHS), diethanolamine, ethyl acrylate, zinc acetate and other chemicals were purchased from Sigma-Aldrich and used without further purification. Near Infra Red dye (DiI – D282) and 4', 6-diamidino-2-phenylindole (DAPI – D1306) were purchased from Invitrogen, whereas the EDC (1-Ethyl-3-[3-dimethylaminopropyl] carbodiimide hydrochloride) was obtained from Pierce Biotechnology. The human lung carcinoma cell line A549 [folate receptor (FR) positive] and breast carcinoma cell line MCF 7 [folate receptor (FR) negative] were obtained from ATCC. Dialysis membranes were obtained from Spectrum Laboratories. Absolute ethanol, chloroform and other solvents were purchased from Fisher Scientific and used as received, unless otherwise stated.

### Methods

Infrared spectra were recorded on a PerkinElmer Spectrum 100 FT-IR spectrometer. UV/Vis spectra were recorded using CARY 300 Bio UV/Vis spectrophotometer. Fluorescence spectra were recorded on a NanoLog Horiba jobin Yvon fluorescence spectrophotometer. NMR spectra were recorded on a Varian 400 MHz spectrometer using the TMS/solvent signal as an internal reference. Gel permeation chromatography (GPC) results were obtained using a JASCO MD 2010 Plus instrument with a PD 2020 light scattering Precision Detector. Thermo gravimetric analyses (TGA) were performed on a SETARAM, Mettler TC11 instrument with sample sizes 10–20 mg. All the experiments were done using a heating rate of 10 °C/min in air. The overall surface charge (zeta potential) of the HBPH nanoparticles was measured using a Zetasizer Nano ZS from Malvern Instruments. Confocal images were taken on a Zeiss Axioskop 2 mot plus confocal microscope. MTT study and BCA assay has been performed using the Synergy μQuant microtiter plate reader (Biotek). Dynamic light scattering (DLS) studies were done using a PDDLS/CoolBatch 40T instrument using Precision Deconvolve 32 software.

NIH-PA Author Manuscript

NIH-PA Author Manuscript

NIH-PA Author Manuscript

### Synthesis of 3-[Bis-(2-hydroxy-ethyl)-amino]-propionic acid ethyl ester (3)

Diethanolamine **1** (10.0 g, 95.24 mmol) and ethyl acrylate **2** (10.48 g, 104.76 mmol) were taken in a round bottom flask containing absolute ethanol (100 mL) and were stirred at 45 °C for 5 h. The reaction mixture was concentrated in a rotavapor at 40 °C and then high vacuum was applied to remove excess ethyl acrylate. The final product was purified by flash chromatography using chloroform and methanol mixture (9:1) as the mobile phase. Yield: 14.1 g (72%). $^1$H NMR (400 MHz, $CDCl_3$, δ ppm, J Hz): 1.27 (t, 3H, $J_1$ = 6.96, $J_2$ = 7.32), 2.49 (t, 2H, $J_1$ = 6.96, $J_2$ = 7.32), 2.64 (t, 4H, $J_1$ = 6.22, $J_2$ = 6.59), 2.85 (t, 2H, $J_1$ = 6.95, $J_2$ = 7.33), 3.61 (q, 4H, $J_1$ = 5.86, $J_2$ = 6.95), 4.15 (q, 2H, $J_1$ = 6.95, $J_2$ = 7.32), 5.17 (bs, 2H). IR: 3247 (broad), 2950 (broad), 1733, 1589, 1390, 1196, 1069, 855, 710 $cm^{-1}$.

### Synthesis of the hydrophilic hyperbranched polyhydroxyl (HBPH) polymer (4)

The monomer **3** (0.07 g, 0.3 mmol), triethanolamine (0.05 g, 0.3 mmol) and a catalytic amount of zinc acetate (100:1 molar ratio) were taken in a 10 mL round bottom flask and dried under high vacuum followed by purging with dry nitrogen gas. Then, the flask was slowly heated to 140 °C under argon atmosphere using an oil bath and kept at this temperature for 0.5 h. The monomer **3** (2.0 g, 9.7 mmol) was added to the resulting reaction mixture in excess and continued heating for 4 h at 140 °C. The reaction mixture was evacuated at 0.2 mm/Hg for 3 h, while maintaining the same polymerization temperature. The polymer was purified by dissolving in methanol and re-precipitating the polymer in acetone. The precipitate was then centrifuged, washed with acetone and dried using a high vacuum pump. The resulting polymer was found to be soluble in methanol, DMF, DMSO and in water. Yield: 61%. $^1$H NMR (400 MHz, $D_2O$, δ ppm): 2.45 (bs, 2H), 2.78 (m, 4H), 2.96 (m, 2H), 3.69 (m, 4H). IR: 3328 (broad), 2893 (broad), 1738, 1612, 1459, 1406, 1396, 1199, 1055, 861, 784 $cm^{-1}$. GPC: $M_w$ = 36,400; PDI = 1.4; TGA: 10% weight loss at 170 °C.

### Synthesis of folate-functionalized HBPH polymer 5

The polymer **4** (0.5 g, 0.016 mmol) was dissolved in dry DMF (1 mL) and then 1,1'-carbonyldiimidazole CDI (0.19 g, 1.19 mmol) in dry DMF (0.1 mL) was added drop-wise to the polymer solution. The reaction mixture was incubated for 2 h at room temperature. After 2 h of incubation, aminated folic acid15, 16 (0.57 g, 1.19 mmol) in dry DMF (0.4 mL) was added drop-wise to the reaction mixture and incubated at room temperature for 24 h. The resulting reaction mixture was then precipitated in acetone, centrifuged and dried in a vacuum pump to get the pure folate-functionalized polymer. Yield: 67%. $^1$H NMR (400 MHz, $D_2O$, δ ppm): 2.15 (m, 4H), 2.41 (bs, 2H), 2.69 (m, 4H), 2.91 (bs, 2H), 3.35 (bs, 4H), 4.15 (m, 4H), 4.31 (bs, 2H), 4.45 (bs, 4H), 6.65 (bs, 2H), 7.2 (bs, 2H), 8.5 (s, 1H). IR: 3275 (broad), 2936 (broad), 2874 (broad), 1730, 1643, 1599, 1545, 1474, 1450, 1389, 1306, 1256, 1191, 1103, 1048, 853 $cm^{-1}$.

### Gel Permeation Chromatography (GPC)

The molecular weight of the resulting polymer was determined using Gel Permeation Chromatography (GPC). The average molecular weight was calculated against a polystyrene standard, using HPLC-grade DMF as the mobile phase. For a comparative study between the average molecular weight ($M_w$) and the polymerization time at 140 °C, the samples were taken from the reaction mixture periodically and analyzed by GPC. With increase in time there was an increase in the molecular weight, whereas a dramatic increase in the polymer's molecular weight was observed when high vacuum was applied.

NIH-PA Author Manuscript

NIH-PA Author Manuscript

NIH-PA Author Manuscript

### Thermogravimatric Analysis (TGA)

The thermal stability of the hydrophilic polyesters was determined by thermogravimetric analysis (TGA). The polymers exhibited a moderate thermal stability in air, an important characteristics for a biodegradable polymer. Approximately, 4% reduction of weight was observed at 140 °C due to the loss of volatile compounds (such as $H_2O$, $CHCl_3$ and DMF), before the thermal degradation starts.

### HBPH nanoparticle formulation: Solvent evaporation method

The HBPH polymer (25 mg), and cargo [fluorophores (5 μL, 10 μg/μL), Cyt C (5 μL, 5 μg/μL)] were dissolved in a mixture of polar solvents ($H_2O$: DMF = 5:1) and vortexed for 2 minutes. The resulting polymer mixture was added drop-wise to acetone (4 mL) with constant stirring, driving both the self-assembly and encapsulation of cargo. Since the HBPH polymer is not soluble in acetone, its presence in a mixture of acetone and water would result in the formation of suspended polymeric "nanodroplets". The resulting nano-suspension was ultrasonicated for 3 minutes to get a homogeneous solution. The resulting homogeneous solution was allowed to evaporate at room temperature and then re-dispersed in DI water resulting in a stable suspension of fluorescently labeled Cyt C encapsulating HBPH nanoparticles. These functional HBPH nanoparticles were purified using a PD-10 column and followed by dialysis (MWCO 15–20K) against PBS solution (pH = 7.4). The purified HBPH nanoparticles were stored at 4 °C until further use.

### Determination of the amount of encapsulated Cyt C

To dilutions of dialyzed Cyt C encapsulating HBPH nanoparticles BCA protein assay (Pierce) was performed in order to quantify their Cyt C content in accordance to the manufacturer's protocol. Absorbance was monitored at 562 nm using a Synergy μQuant microtiter plate reader (Biotek).

### Enzyme kinetics of Cyt C-HBPH NP's peroxidase activity

To determine if the Cyt C-HBPH nanoparticles possessed peroxidase activity, aliquots of these nanoparticles with varying Cyt C concentrations were added to 100 μL TMB [1 mg/mL in DMSO:DI $H_2O$ (1:9)], in a 96-well plate. Color formation was observed after addition of 20 μL $H_2O_2$ (0.03%), followed by immediate picture acquisition. For steady-state kinetic studies, serial dilutions of TMB were prepared in citrate buffer (pH 4.0), and 100 μL aliquots were dispensed in a 96-well plate. Subsequently, 5 μL of Cyt C HBPH nanoparticles were added to the corresponding wells, followed by addition of 20 μL $H_2O_2$ (0.03%). Absorbance was recorded at 652 nm using the time-scan mode of the Synergy μQuant 200 microtiter plate reader (Biotek). The kinetic parameters were determined via the Michaelis-Menten equation:

$$v = V_{max} \times [S]/(K_m + [S])$$

where ν is the initial rate of the reaction, $V_{max}$ is the maximum rate of the reaction, [S] is the substrate's concentration, and $K_m$ is the Michaelis constant.

### *In vitro* cell studies

**Cell cultures—**The human lung carcinoma (A549) and breast carcinoma (MCF 7) cells were obtained from ATCC, and maintained in accordance to the supplier's protocols. Briefly, the lung carcinoma cells were grown in a 5%-FBS-containing DMEM medium supplemented with L-glutamine, streptomycin, amphotericin B and sodium bicarbonate. The MCF 7 cells were propagated in a 10% FBS-containing MEM medium containing penicillin,

NIH-PA Author Manuscript

NIH-PA Author Manuscript

NIH-PA Author Manuscript

streptomycin and bovine insulin (0.01 mg/mL). Cells were grown in a humidified incubator at 37 °C under 5% $CO_2$ atmosphere.

**MTT assay—**MCF 7 cells (2,500 cells/well) were seeded in 96-well plates and incubated with Cyt C-HBPH nanoparticles (3.2 mg/mL) for 6 h at 37 °C. Then, each well was washed three times with 1× PBS and treated with 20 μL MTT (5 μg/μL) for 2 h. The resulting formazan crystals were dissolved in acidic isopropanol (0.1 N HCl) and the absorbance was recorded at 570 and 750 nm (background), using a Synergy μQuant microtiter plate reader (Biotek). These experiments were performed in triplicates.

**Confocal laser-scanning microscopy—**MCF 7 and A549 cells (10,000) were incubated with the corresponding functional Cyt C-HBPH nanoparticle preparations (3.2 mg/mL) for 6 h in a humidified incubator (37 °C, 5% $CO_2$). Subsequently, the cells were thoroughly washed three times with 1× PBS, fixed with 10% formalin solution and visualized via confocal imaging using a Zeiss LSM 510 confocal microscope equipped with 20× and 40× objectives. For detection of apoptosis-dependent nuclear fragmentation, the supernatant of the treated cells (which contain floating apoptotic cells) was incubated with propidium iodide (PI, 50 μg/mL), followed by nuclear staining with DAPI. The nuclei of the permeable apoptotic cells are seen as a bright purple in confocal microcopy, due to co-localization of PI and DAPI, with highly condensed and fragmented chromatin, as previously reported.[17, 18]

**IVIS analysis—**A549 and MCF 7 cells (10,000) were incubated for 6 h with the corresponding ICG-containing Cyt C-HBPH nanoparticles (3.2 mg/mL). At the end of the incubation period, the supernatant was collected in eppendorf tubes and the cells were thoroughly washed with 1× PBS and detached, as stated above. The resulting pellets were resuspended in 1 mL culture media. All eppendorf tubes were examined simultaneously on a Xenogen IVIS system, using the ICG filter for ICG dye.

**In vitro Cyt C release—**I*n vitro* Cyt C release studies were carried out using a dynamic dialysis technique at 37 °C. Briefly, 100 μL of Cyt C-HBPH nanoparticles (3.2 mg/mL) were incubated with porcine liver esterase (20 μL, 850 units/mL) inside a dialysis bag (MWCO 15–20k), which was then placed in a PBS solution (pH 7.4). The amount of Cyt C released from the nanoparticle into the PBS solution was determined at regular time intervals by taking 1 mL aliquots from the PBS solution and measuring absorbance at 409 nm (soret band) of Cytochrome c. A similar experiment was performed at pH 4.0 instead of using esterase enzyme. The concentration of the Cyt C was calculated using a standard calibration curve. The cumulative fraction of release versus time was calculated using the following equation:

$$\text{Cumulative release } (\%) = [\text{Cyt C}]_t / [\text{Cyt C}]_{\text{total}} \text{ X } 100$$

Where $[\text{Cyt C}]_t$ is the amount of Cyt C released at time t, $[\text{Cyt C}]_{\text{total}}$ is the total Cyt C present in the Cyt C-encapsulating nanoparticles.

## Results

### Design, synthesis and characterization of HBPH polymer

Synthesis of the water-soluble hyperbranched polyhydroxyl (HBPH) polymer was achieved from a water-soluble $AB_2$ type monomer [3-{Bis-(2-hydroxy-ethyl)-amino}-propionic acid ethyl ester, **3**] having a tertiary nitrogen atom in the structure with three-bond connectivity. The monomer was synthesized following a typical Michael-addition reaction,[19, 20] where

NIH-PA Author Manuscript

NIH-PA Author Manuscript

NIH-PA Author Manuscript

diethanolamine in ethanol was reacted with ethyl acrylate for 5 h at 45 °C (scheme 1). The monomer with a tertiary nitrogen atom at the branching point yielded three-dimensional polyhydroxyl-based hyperbranched polyester **4** upon melt-polymerization.21 The use of a trifunctional core molecule, triethanolamine, during the initial polymerization reaction was important to minimize the syntheses of undesired cross-linked polymers and low molecular weight oligomers. This aliphatic HBPH polymer was purified using a precipitation method, where the polymer was dissolved in methanol and precipitated in acetone, as the crude polymer was found to be insoluble in acetone. The resulting pure polymer was dried under high vacuum and found to be soluble in water, methanol and DMF. The monomer and the HBPH polymer were characterized by $^1$H NMR and FTIR spectroscopic analysis (SI Figure S1 and Figure S2). The molecular weight of the polymer **4** was determined using Gel Permeation Chromatography (GPC) and showed the formation of a high molecular weight polymer (Figure 1A, $M_w$ = 36,400, PD = 1.4). Thermal gravimetric analysis (TGA) of **4** showed moderate thermal stability (10% weight loss at 170 °C in air), demonstrating the amorphous nature of our polymer (SI Figure S3).22 The moderate thermal stability, highly branched nature and the presence of ester linkages in the three dimensional polymeric backbone make this HBPH polymeric nanoparticle biodegradable by various intracellular esterases. As shown in Scheme 1, the HBPH polymer (**4**) contains aliphatic segments with hydroxyl and tertiary amine groups, potentially facilitating the encapsulation of diverse guest molecules, through weak electrostatic and hydrogen bonding interactions. In addition, our polyhydroxyl polymer, contrary to the conventional linear polymers, is three-dimensional, water soluble, and contains numerous surface hydroxyl functional groups, suggesting its targetability and versatility in biomedical applications.

## Preparation and characterization of Cyt C-HBPH nanoparticles

Stable and dispersed Cytochrome c encapsulating HBPH nanoparticles (Cyt C-HBPH NPs) were synthesized using the solvent evaporation method.22 We utilized this nanoparticle preparation method, as opposed to the solvent diffusion method, because our polymer and cargos were water-soluble. Furthermore, this method does not use any emulsifiers or denaturing solvents, thus preventing protein denaturation. In addition, we co-encapsulated a fluorophore (DiI or ICG) to label the nanoparticle and facilitate its tracking and localization within the cell and potentially *in vivo*. In brief, the HBPH polymer and cargo (Cyt C and fluorophore) were dissolved in a mixture of polar solvents ($H_2O$: DMF = 5:1) and added drop-wise to acetone with constant stirring, driving both the self-assembly and encapsulation of cargo. Since the HBPH polymer is not soluble in acetone, its presence in a mixture of acetone and water would result in the formation of suspended polymeric "nanodroplets" that upon ultrasonication, subsequent solvent evaporation and re-dispersion in water resulted in a stable suspension of fluorescently labeled Cyt C encapsulating HBPH nanoparticles in water. In this method, the miscible solvents ($H_2O$ and DMF) rapidly diffuse into acetone, causing the polymer to self-assemble, bringing the amphiphilic areas together and therefore creating amphiphilic cavities that encapsulate Cyt C and the fluorophore, while exposing hydrophilic functional groups towards the surface of the nanoparticle.

Dynamic Light Scattering (DLS) experiment of Cyt C-HBPH nanoparticles, confirmed the presence of stable and monodispersed nanoparticles with hydrodynamic diameter of 63±2 nm (Figure 1B). Encapsulation of Cyt C inside the HBPH polymer cavity was confirmed by performing UV/Vis spectroscopic experiments and observing a red shift of 5 nm (Figure 1C) in the Cyt C encapsulating HBPH nanoparticles (414 nm) compared to the free Cyt C in solution. The amount of encapsulated Cyt C in the HBPH nanoparticles preparation (0.71 μg of protein/mL) was determined using standard BCA assay. We observed that the loading efficiency of the Cyt C into the polymeric cavity was dependent on the concentration of the Cyt C solutions used for encapsulation. This observation indicated that the encapsulation

NIH-PA Author Manuscript

NIH-PA Author Manuscript

NIH-PA Author Manuscript

was a diffusion driven process and reached maximum loading once the polymeric cavities were saturated.

In order to evaluate Cyt C's integrity within the nanoparticles and to assess that the enzyme is still enzymatically active after encapsulation, we examined the peroxidase enzymatic activity of the Cyt C-HBPH nanoparticles. The peroxidase activity of Cytochrome c is a known enzymatic activity of the native protein. The results of the Cyt C-HBPH nanoparticle's kinetics studies revealed that they do exhibit Michaelis – Menten kinetics, with a $V_{max}$ comparable to that of other peroxidase-mimicking nanoparticles (Figure 2A).[23–25] Furthermore, the Cyt C-HBPH nanoparticles were able to rapidly oxidize a widely used chromogenic peroxidase substrate, 3,3',5,5'-tetramethylbenzidine (TMB), hinting the potential use of these nanoparticles in immunoassays and *in vitro* diagnostics (Figure 2B). Overall, these findings corroborated the hypothesis that our HBPH polymer can effectively encapsulate therapeutic proteins, such as Cyt C, without compromising their stability and intrinsic enzymatic properties.

For optimal therapeutic applications, not only a stable encapsulation of Cyt C within the HBPH nanoparticle cavities has to be achieved, but also a selective release of the protein must occur upon cell internalization. The selective release of Cyt C into the cytoplasm of cancer cells would result in the induction of apoptosis of such cells. Towards this direction, we investigated if the Cyt C-HBPH nanoparticle can retain its therapeutic cargo at physiological pH (7.4) for a long period of time, but selectively release its cargo in an acidic microenvironment or by the action of an esterase at physiological pH. For these studies, the Cyt C-HBPH nanoparticles were incubated in PBS and the rate of cargo release was measured by the dialysis method as described in our previous work.[14, 16] The presence of Cyt C in the aqueous media outside the dialysis bag was determined by measuring the UV/Vis absorption profile of the Cyt C's Soret band (409 nm) in the buffer. Results showed that no significant release of Cyt C was observed upon incubation at physiological pH (7.4) (Figure 3A–B). Similar results were obtained upon prolonged incubation for up to one week. In addition, DLS studies of the nanoparticle preparation showed no alteration of the nanoparticle's size distribution during the incubation period at pH 7.4. Control experiments also confirmed the absence of enzymatically active Cyt C in the aqueous media of Cyt C-HBPH nanoparticles at pH 7.4, due to the absence of TMB oxidation (Figure 3C). Taken together, these results indicate that the Cyt C-HBPH nanoparticles were stable at physiological pH over a prolonged time, without undergoing any cargo release due to nonspecific degradation of the polymeric nanoparticle. However, in the presence of an esterase or acidic pH (pH 4.0) the nanoparticles gradually released Cyt C, achieving total payload delivery within 5 h (Figure 3A–B). Additionally, we examined whether the acidic microenvironment or the presence of the esterase affected the enzymatic activity of Cyt C, plausibly due to structural alterations that may have led to loss of its heme. Interestingly, we found that the released Cyt C was still enzymatically active rapidly oxidizing TMB, regardless of the release trigger (pH 4 or esterase) (Figure 3C). Overall, these results indicated that upon HBPH nanoparticle encapsulation, Cyt C was still in a native conformation and enzymatically active form, even after its release due to stimulated nanoparticle degradation.

### HBPH nanoparticle uptake and their cytotoxic effect in cancer cell

In subsequent studies, we investigated whether the Cyt C-HBPH nanoparticles were able to release active Cyt C upon cellular uptake and induce apoptosis in these cells. In our first set of experiments, we incubated MCF 7 breast carcinoma cells with the nanoparticles for 6 h at 37 °C 5% $CO_2$, followed by total cell isolation. After isolation, the cells pellets were resuspended in TMB (1 mg/mL), followed by addition of hydrogen peroxide (0.03 %). Spectrophotometric measurements revealed that the MCF 7 cells treated with Cyt C-HBPH

NIH-PA Author Manuscript

NIH-PA Author Manuscript

NIH-PA Author Manuscript

nanoparticles had a significant absorbance at 652 nm, attributed to the oxidation of TMB by the Cyt C's intrinsic peroxidase-like activity (Figure 4A). On the other hand, the untreated MCF 7 cells exhibited minimal absorbance, most likely due to the presence of low levels of endogenous Cyt C found within the mitochondria. Visual confirmation of the oxidation of TMB oxidation in the suspension of cells treated with Cyt C-HBPH nanoparticles was also achieved within 30 minutes after addition of hydrogen peroxide, as indicated by the presence of a pale blue color (Figure 4B). Hence, these findings suggest that the Cyt C-HBPH nanoparticles can deliver and release enzymatically active Cyt C to MCF 7 cells.

Next, we investigated whether the Cyt C-HBPH nanoparticles (3.2 mg/mL) could induce apoptosis, due to the intracellular release of the protein. After a 6 h long incubation at 37 °C, results indicated that there was a significant reduction in the viability of MCF 7 cell treated with the Cyt C encapsulating nanoparticles (Figure 5). In order to confirm that Cyt C was the modulator of the observed decreased cell viability and not the HBPH polymer, we incubated cells with unloaded HBPH nanoparticles, containing no cargo (either Cyt C or dye). As there was absence of cytotoxicity in these cells (Figure 5), we concluded that Cyt C, and not the non-encapsulated nanoparticle (HBPH), facilitates the observed cell death presumably due to the induction of apoptosis upon the Cyt C intracellular release. Microscopic examination of the MCF 7 cells in culture corroborated the cell viability data, indicating that both the untreated and HBPH nanoparticles treated cells had normal morphology with few cells floating (dead cells) in the culture medium (Figure 6). In contrast, the cells treated with Cyt C-HBPH nanoparticles had abnormal morphology with a significant number of floating, and presumably apoptotic cells.

To confirm that the floating cells were indeed apoptotic, we assessed the presence of nuclear segmentation and chromatin condensation in their nuclei using a previously published methodology.17, 18 Specifically, this microscopic method relies on the distinct morphological patterns in the nucleus of apoptotic cells, upon staining with propidium iodide (PI) and DAPI. In apoptotic cells, both dyes PI (red) and DAPI (blue) will localize to the nucleus due to presence of pores on the cell membrane. Upon incubation of the floating cells with both PI and DAPI for 6 h it was found that both dyes localized to the nucleus as judged by the presence of a purple nuclei. Furthermore, extensive heterogeneous chromatin condensation and nuclear fragmentation was observed in the nucleus of these cells (Figure 7), suggesting ongoing apoptosis. Taken together, these results indicate that the HBPH nanoparticles can efficiently encapsulate a protein, such as Cyt C, and induce apoptosis upon internalization in breast carcinomas MCF 7.

### Targeted delivery of Cyt C-HBPH nanoparticles to cancer cells

The cancer therapeutic ability of the Cyt C-HBPH nanoparticles could be enhanced by endowing these nanoparticles with the ability to specifically target cancer cells, while avoiding healthy cells. To explore this potential application, we conjugated our HBPH polymer with folic acid as a model system. Folic acid is the known ligand for the folate receptor which has been found to be overexpressed in most cancer cells and has been widely used as a model for addressing the targetability of imaging and therapeutic agents. The surface hydroxyl groups of the HBPH polymer were conjugated with aminated folic acid using carbodiimide chemistry (SI Scheme S1). Briefly, 1,1'-Carbonyldiimidazole (CDI) was dissolved in dry DMF containing HBPH polymer (**4**) and followed by addition of aminated folic acid15, 16 an subsequent incubation for 2 h at room temperature. The resulting folate conjugated polymer (**5**) was purified and then characterized by spectroscopic analysis (SI Figure S4). To track the localization of the HBPH nanoparticles within the cells, a DiI dye was encapsulated along with the Cyt C protein using the solvent evaporation method and characterized by spectroscopic experiments (Figure 1D, SI Figure S5) after purification.

NIH-PA Author Manuscript

NIH-PA Author Manuscript

NIH-PA Author Manuscript

First, we evaluated the selective internalization of our DiI encapsulating folate-conjugated HBPH nanoparticles (Fol-DiI-HBPH NPs) by lung cancer cells (A549) which overexpress the folate receptor.14, 26, 27 As a negative control, we used breast cancer cells (MCF 7), which do not express the folate receptor.28 In these set of experiments, the folate-nanoparticles (3.2 mg/mL, Fol-DiI-HBPH NPs) were incubated with the above mentioned cell lines (10,000 cells) for 6 h, washed with PBS to remove non-internalized nanoparticles and visualized using confocal microscopy. Results showed an enhanced fluorescence in the cytoplasm of A549 cells (Figure 8A–C), whereas no significant internalization was observed in MCF 7 cells (Figure 8J–L). In another set of experiment, the internalization of the Fol-DiI-HBPH nanoparticles was found to be minimal in the same cancer cells (A549) when pre-incubated with free folic acid (Figure 8D–F). These experiments confirmed the selective folate-receptor-mediated internalization of our folate conjugated HBPH nanoparticles only by the cancer cells that overexpress folate receptor. Interestingly, when lung carcinoma A549 cells were incubated with the the Cyt C encapsulating HBPH nanoparticles (Fol-Cyt C/DiI-HBPH NPs) a significant induction of cell apoptosis was observed, leading to dramatic cellular morphological changes and cell death (Figure 8G–I). This observation supported our hypothesis that the Cyt C's therapeutic efficacy was preserved, despite its nanoparticle encapsulation and it was possible to specifically target and kill the cancer cells using our folate conjugated nanoparticles containing Cyt C (Fol-Cyt C/DiI-HBPH NPs). Taken together, these findings support the principle that folate-functionalized HBPH nanoparticles can be used to target and deliver chemotherapeutic agents to folate-receptor-overexpressing carcinomas, achieving specific delivery and monitoring of the therapeutic regime.

The targeted induction of apoptosis in the folate receptor expressing A549 lung cancer cells was further confirmed by staining the treated cells with DAPI and PI. Results showed induction of apoptosis by observing the presence of heterogeneous chromatin condensation and nuclear fragmentation in the A549 cells (Figure 9A), contrary to the MCF 7 cells (Figure 9B) upon treatment with the Fol-Cyt C-HBPH nanoparticles. These results strongly support the importance of encapsulating therapeutic protein within the polymeric cavity and targeting its delivery, in order to prevent damage of non-transformed cells and healthy tissues. Therefore, folate-conjugated HBPH nanoparticles, compared to their non-folate counterparts, can specifically deliver a protein such as cytochrome c to folate expressing cancer cells inducing apoptosis.

For *in vivo* imaging applications, nanoparticles with excitation and emission in the near infrared region (650–900 nm) are needed for deep tissue fluorescence imaging. The dialkylcarbocyanine dye ICG is of particular clinical importance, since it has an excitation/emission in the near infrared region (751/780 nm) and it is already used for *in vivo* imaging and determination of cardiac output and hepatic function, among others.29, 30 Towards this end, we encapsulated ICG and Cyt C into the folate-conjugated HBPH polymer (**5**), following the solvent evaporation method. UV/Vis and fluorescence studies (Figure 10) confirmed the presence of the near infrared ICG dye and Cyt C inside the polymer cavities. To demonstrate the targeting and *in vivo* imaging capabilities of our near-infrared folate-functionalized HBPH nanoparticles (Fol-ICG-HBPH NPs), A549 cells (FR positive) and MCF 7 cells (FR negative, 10,000 cells) were treated with the folate nanoparticles (3.2 mg/mL) for 6 h. Next, the cells were washed with PBS and detached with trypsin. After centrifugation, the resulting cell pellets were simultaneously imaged using an indocyanine green (ICG) filter in an *In Vitro* Imaging System (IVIS). No cell-associated near infrared fluorescence was observed in MCF 7 cells (Figure 11A), whereas a dose-dependent cell-associated ICG fluorescence was observed in A549 cells (Figure 11B). Since the cells were extensively washed with PBS before imaging and considering the confocal microscopy results shown in Figure 8, these findings support that our protein loaded theranostic

NIH-PA Author Manuscript

NIH-PA Author Manuscript

NIH-PA Author Manuscript

nanoparticle can be used for the *in vivo* imaging and targeted transmembrane delivery of the therapeutic agents.

## Discussion

Current cancer chemotherapeutic regimes are associated with severe side-effects, including renal toxicity and immune-suppression. In principle, these effects arise from the lack of specificity of the chemotherapeutic agents, as their systemic administration results in their rapid and extensive bio-distribution, without discrimination of healthy tissue versus neoplastic lesions.[31, 32] Hence, due to the drugs' high toxicity, normal tissue is adversely affected as well. At the same time, cancer cells within a tumor may not uptake these agents, due to their short stay in circulation or low local concentrations in the tumor's vicinity, potentially leading to tumor re-growth and metastasis.[33, 34] For these reasons, newer chemotherapeutic agents with increased selectivity are needed, particularly drugs that employ molecular mimicry to bind to tumor-specific transmembrane receptors.[35] Current therapies with anticancer small drugs are affected by the rapid clearance of the drug from the body and the ability of cancer cells to adopt diverse drug resistance mechanisms, including epitope alteration and expression of efflux pumps among others.[12] Although alternative strategies, such as photodynamic therapy and hyperthermia, can frequently be targetable, they facilitate tumor regression via necrotic mechanisms.[36–39] The leakage of intracellular components to the extracellular milieu during necrosis promotes extensive inflammation and accumulation of toxic byproducts to the proximity of healthy cells. Therefore, these cancer therapies, although potent, are associated with the bystander effect, where the treatment process and the subsequent necrotic cascade cause adjacent healthy tissue damage.

Contrary to necrosis, apoptosis is the physiological process where intracellular components are degraded by lytic enzymes, within membrane bound components.[7, 8] Through apoptosis, the cell can break down its components to less complex by-products, which can readily undergo clearance by lymphocytes and macrophages with minimal deleterious effects to the healthy surrounding tissue. During development and throughout an organism's life, apoptosis plays a critical role, preserving proper cell function. Triggers of apoptosis include irreparable genome damage, cytoskeletal alterations and loss of cell adhesion among others. A critical apoptotic event for the activation of downstream lytic enzymes is the release of Cytochrome c from the mitochondrial inter-membrane locus to the cytoplasm. Although cancer cells have developed mechanisms to inhibit this event, cytoplasmic delivery of Cytochrome c at adequate levels can effectively induce apoptosis and potentially lead to tumor regression, without affecting non-cancerous cells.[4] In order to achieve cytoplasmic delivery of Cyt C, it is desirable to encapsulate the protein within polymeric entities, which can be targetable. In this report, a water-soluble hyperbranched polyhydroxyl (HBPH) polymer was synthesized from a diethanolamine-derived $AB_2$ monomer, where the monomer was synthesized following a typical Michael-addition reaction. The presence of aliphatic hydroxyl groups and a tertiary nitrogen atom, as well as the monomer's structure conferring 'three-bond connectivity', are important components of the three-dimensional HBPH polymer. The synthesized crude HBPH polymer was found to be soluble in water, methanol and DMF, whereas it was insoluble in acetone. This property of the HBPH polymer facilitated its purification by precipitation in acetone. The synthesized globular structured HBPH polymer has many advantages over conventional linear polymers, including water solubility, presence of cavities for effective encapsulation of diverse cargos (dyes, proteins, DNA, RNA, drugs and other therapeutics) and large number of surface-occupying hydroxyl groups for solubility and targetability.

Therefore, our HBPH polymer is an ideal building block for the formation of nanoparticles and encapsulation of large quantities of diverse cargos within its amphiphilic cavities. The

NIH-PA Author Manuscript

NIH-PA Author Manuscript

NIH-PA Author Manuscript

presence of aliphatic chains, ester groups, tertiary nitrogen atoms and hydroxyl groups in the polymer core made the cavities amphiphilic in nature and capable of encapsulating a variety of amphiphilic cargos. Thermogravimetric analysis showed moderate thermal stability of the polymer, indicating that our polymer was amorphous. In addition, cytotoxicity studies showed that the non-encapsulated nanoparticles were non-toxic, demonstrating biocompatibility of our synthesized HBPH polymer. An important feature of the resulting cargo-encapsulating HBPH nanoparticles is their stability in PBS (pH = 7.4), which prevents the payload's constitutive release to the aqueous milieu. This is highly desired as the traceable cargo is released only in the presence of esterases and acidic pH, which are found in endocytic vesicles upon receptor-mediated cellular uptake. Plausibly, the HBPH nanoparticles can be used for the controlled release of therapeutics to specific disease loci, such as the acidified microenvironment of carcinomas that arises from the Warburg effect and enhanced glycolysis.

The use of the solvent evaporation method was effective for the formulation of nanoparticles and encapsulation of various cargos, due to the presence of unique electrostatic interactions between the cargo and the functional polymeric backbone. Our results indicate that the HBPH nanoparticles preserved Cyt C's properties, as indicated by their peroxidase and apoptotic activities. A principal reason for maintaining the protein's activities was the nature of the polymer and the employed nanoparticle preparation method, as the latter does not incorporate any surfactants or denaturing conditions. Hence, the Cyt C-loaded HBPH nanoparticles behaved as a peroxidase mimetic, being able to oxidize TMB in the presence of hydrogen peroxide. Notably after cellular uptake, the Cyt C HBPH nanoparticles still exhibited peroxidase-mimicking activity only upon $H_2O_2$ supplementation. Furthermore, microscopic examinations revealed that the uptake of these nanoparticles effectively induced apoptosis, suggesting the use of these nanoparticles for the potential targeted controlled release of an endogenous therapeutic to malignant and diseased cells.

To achieve the receptor-mediated endocytic uptake in cancer cells, we conjugated folic acid to the hydroxyl groups of our polymer, making it a targetable therapeutic and diagnostic vehicle. The folate-conjugated Cyt C-HBPH nanoparticles induced apoptosis in folate-receptor-positive lung carcinoma cells (A549). However, no folate-carrying nanoparticle uptake or apoptosis were observed in cells lacking the folate receptor (MCF 7), suggesting the specificity of the nanoparticles' cytotoxic potency. We adopted folic acid as the nanoparticles' targeting moiety, because (i) the folate receptor is overexpressed in various carcinomas and metastatic lesions, (ii) folic acid analogs are already used in the clinic as folate-receptor-binding drugs (i.e. methotrexate) and (iii) folic acid-conjugated probes are in clinical trials for cancer imaging, such as folate-conjugated radioisotopes and nanoparticles.[40–44] However, apart from folic acid, other targeting ligands may be conjugated as well.

In addition to the targeted delivery of Cytochrome c and the initiation of apoptosis, the HBPH nanoparticles can be used for the monitoring of the therapeutic regime, the assessment of tumor regression and the localization of the nanoparticles *in vivo*.[45, 46] Hence obtaining this information, a physician may tailor the therapeutic regime without using invasive methodologies, while utilizing an endogenous apoptotic initiator and abolishing any side-effects associated with current chemotherapy. Furthermore, these nanoparticles may be used for the *in vitro* determination of the expression of cancer biomarkers found on the plasma membrane of tumoric cells, utilizing HBPH Cytochrome c nanoparticles' peroxidase-like activity.

NIH-PA Author Manuscript

NIH-PA Author Manuscript

NIH-PA Author Manuscript

## Conclusion

In summary, we have introduced a new water soluble hyperbranched polyhydroxyl (HBPH) nanoparticle capable of encapsulating small membrane-impermeable proteins, such as Cytochrome c and near infrared dyes for a potential target-specific detection and treatment of tumors. The presence of amphiphilic pockets inside the three dimensional hyperbranched structures played an important role in the encapsulation of a variety of cargos, such as fluorescent dyes and a protein, using the solvent evaporation method. The resulting functional polymeric nanoparticles were stable in aqueous buffered solutions, has good cellular targeting ability and their simple synthesis process is amenable to scale-up. Our studies demonstrated that either an enzyme (esterase) or acidic pH can trigger the release of the protein from the polymeric cavities. Similar to the native Cytochrome c, the protein released from the HBPH nanoparticles core could also function as an active enzyme in oxidation reactions in aqueous media. Furthermore, when conjugated with folic acid, the protein-encapsulating HBPH nanoparticles could serve as targeted transmembrane carriers, delivering Cyt C to cancer cells that overexpress the folate receptor and inducing apoptosis. The intracellular release of Cyt C and cell apoptosis were confirmed optically using confocal microscopy. This offers the possibility to create a library of novel multifunctional polymeric materials with unique properties that can be tailored by the nature of their cargo and their surface functionality. Concluding, the development of these HBPH nanoparticle-based targeted release systems may lead to breakthroughs in therapeutic and diagnostic applications.

## Supplementary Material

Refer to Web version on PubMed Central for supplementary material.

## Acknowledgments

This work was supported by the NIH grant GM 084331 to JMP. We thank Dr. Steven Ebert (University of Central Florida) for his assistance with the IVIS studies.

## References

1. Lynn DM, Anderson DG, Putnam D, Langer R. Accelerated discovery of synthetic transfection vectors: parallel synthesis and screening of a degradable polymer library. J. Am. Chem. Soc. 2001; 123(33):8155–8156. [PubMed: 11506588]
2. Shenoy D, Little S, Langer R, Amiji M. Poly(ethylene oxide)-modified poly(beta-amino ester) nanoparticles as a pH-sensitive system for tumor-targeted delivery of hydrophobic drugs. 1. In vitro evaluations. Mol. Pharm. 2005; 2(5):357–366. [PubMed: 16196488]
3. Soppimath KS, Aminabhavi TM, Kulkarni AR, Rudzinski WE. Biodegradable polymeric nanoparticles as drug delivery devices. J. Control Release. 2001; 70(1–2):1–20. [PubMed: 11166403]
4. Slowing II, Trewyn BG, Lin VSY. Mesoporous silica nanoparticles for intracellular delivery of membrane-impermeable proteins. J. Am. Chem. Soc. 2007; 129(28):8845–8849. [PubMed: 17589996]
5. Kam NW, Dai H. Carbon nanotubes as intracellular protein transporters: generality and biological functionality. J. Am. Chem. Soc. 2005; 127(16):6021–6026. [PubMed: 15839702]
6. Kam NW, Liu Z, Dai H. Carbon nanotubes as intracellular transporters for proteins and DNA: an investigation of the uptake mechanism and pathway. Angew. Chem. Int. Ed. Engl. 2006; 45(4):577–581. [PubMed: 16345107]
7. Green DR, Reed JC. Mitochondria and apoptosis. Science. 1998; 281(5381):1309–1312. [PubMed: 9721092]

NIH-PA Author Manuscript

NIH-PA Author Manuscript

NIH-PA Author Manuscript


8. Hengartner MO. The biochemistry of apoptosis. Nature. 2000; 407(6805):770–776. [PubMed: 11048727]
9. Cao X, Bennett RL, May WS. c-Myc and caspase-2 are involved in activating Bax during cytotoxic drug-induced apoptosis. J. Biol. Chem. 2008; 283(21):14490–14496. [PubMed: 18375382]
10. Jurgensmeier JM, Xie Z, Deveraux Q, Ellerby L, Bredesen D, Reed JC. Bax directly induces release of cytochrome c from isolated mitochondria. Proc. Natl. Acad. Sci. U S A. 1998; 95(9): 4997–5002. [PubMed: 9560217]
11. Rosse T, Olivier R, Monney L, Rager M, Conus S, Fellay I, Jansen B, Borner C. Bcl-2 prolongs cell survival after Bax-induced release of cytochrome c. Nature. 1998; 391(6666):496–499. [PubMed: 9461218]
12. Dubrez-Daloz L, Dupoux A, Cartier J. IAPs: more than just inhibitors of apoptosis proteins. Cell Cycle. 2008; 7(8):1036–1046. [PubMed: 18414036]
13. Pilkington GJ, Parker K, Murray SA. Approaches to mitochondrially mediated cancer therapy. Semin. Cancer Biol. 2008; 18(3):226–235. [PubMed: 18203619]
14. Santra S, Kaittanis C, Perez JM. Aliphatic hyperbranched polyester: a new building block in the construction of multifunctional nanoparticles and nanocomposites. Langmuir. 2010; 26(8):5364–5373. [PubMed: 19957939]
15. Riebeseel K, Biedermann E, Loser R, Breiter N, Hanselmann R, Mulhaupt R, Unger C, Kratz F. Polyethylene glycol conjugates of methotrexate varying in their molecular weight from MW 750 to MW 40000: synthesis, characterization, and structure-activity relationships in vitro and in vivo. Bioconjug. Chem. 2002; 13(4):773–785. [PubMed: 12121133]
16. Santra S, Kaittanis C, Grimm J, Perez JM. Drug/dye-loaded, multifunctional iron oxide nanoparticles for combined targeted cancer therapy and dual optical/magnetic resonance imaging. Small. 2009; 5(16):1862–1868. [PubMed: 19384879]
17. Lee Y, Shacter E. Bcl-2 does not protect Burkitt's lymphoma cells from oxidant-induced cell death. Blood. 1997; 89(12):4480–4492. [PubMed: 9192772]
18. Shacter E, Williams JA, Hinson RM, Senturker S, Lee YJ. Oxidative stress interferes with cancer chemotherapy: inhibition of lymphoma cell apoptosis and phagocytosis. Blood. 2000; 96(1):307–313. [PubMed: 10891466]
19. Akinc A, Anderson DG, Lynn DM, Langer R. Synthesis of poly(beta-amino ester)s optimized for highly effective gene delivery. Bioconjug. Chem. 2003; 14(5):979–988. [PubMed: 13129402]
20. Akinc A, Lynn DM, Anderson DG, Langer R. Parallel synthesis and biophysical characterization of a degradable polymer library for gene delivery. J. Am. Chem. Soc. 2003; 125(18):5316–5323. [PubMed: 12720443]
21. Santra S, Kumar A. Facile synthesis of aliphatic hyperbranched polyesters based on diethyl malonate and their irreversible molecular encapsulation. Chem. Commun. 2004; (18):2126–2127.
22. Kietzke T, Neher D, Landfester K, Montenegro R, Guntner R, Scherf U. Novel approaches to polymer blends based on polymer nanoparticles. Nat. Mater. 2003; 2(6):408–412. [PubMed: 12738959]
23. Nath S, Kaittanis C, Ramachandran V, Dalal N, Perez JM. Synthesis, magnetic characterization and sensing applications of novel dextran-coated iron oxide nanorods. Chem. Mater. 2009; 21(8): 1761–1767. [PubMed: 20204168]
24. Perez JM. Iron oxide nanoparticles: hidden talent. Nat. Nanotechnol. 2007; 2(9):535–536. [PubMed: 18654361]
25. Asati A, Santra S, Kaittanis C, Nath S, Perez JM. Oxidase-like activity of polymer-coated cerium oxide nanoparticles. Angew. Chem. Int. Ed. Engl. 2009; 48(13):2308–2312. [PubMed: 19130532]
26. Yuan H, Miao J, Du YZ, You J, Hu FQ, Zeng S. Cellular uptake of solid lipid nanoparticles and cytotoxicity of encapsulated paclitaxel in A549 cancer cells. Int. J. Pharm. 2008; 348(1–2):137–145. [PubMed: 17714896]
27. Nelson ME, Loktionova NA, Pegg AE, Moschel RC. 2-amino-O4-benzylpteridine derivatives: potent inactivators of O6-alkylguanine-DNA alkyltransferase. J. Med. Chem. 2004; 47(15):3887–3891. [PubMed: 15239666]
28. Chung KN, Saikawa Y, Paik TH, Dixon KH, Mulligan T, Cowan KH, Elwood PC. Stable transfectants of human MCF-7 breast cancer cells with increased levels of the human folate

NIH-PA Author Manuscript

NIH-PA Author Manuscript

NIH-PA Author Manuscript

receptor exhibit an increased sensitivity to antifolates. J. Clin. Invest. 1993; 91(4):1289–1294. [PubMed: 7682567]

29. Iriyama A, Uchida S, Yanagi Y, Tamaki Y, Inoue Y, Matsuura K, Kadonosono K, Araie M. Effects of indocyanine green on retinal ganglion cells. Invest. Ophthalmol. Vis. Sci. 2004; 45(3): 943–947. [PubMed: 14985315]
30. Yaseen MA, Yu J, Jung B, Wong MS, Anvari B. Biodistribution of encapsulated indocyanine green in healthy mice. Mol. Pharm. 2009; 6(5):1321–1332. [PubMed: 19799463]
31. Adcock IM, Ito K. Molecular mechanisms of corticosteroid actions. Monaldi. Arch. Chest. Dis. 2000; 55(3):256–266. [PubMed: 10948677]
32. Brana MF, Cacho M, Gradillas A, de Pascual-Teresa B, Ramos A. Intercalators as anticancer drugs. Curr. Pharm. Des. 2001; 7(17):1745–1780. [PubMed: 11562309]
33. Panyam J, Labhasetwar V. Sustained cytoplasmic delivery of drugs with intracellular receptors using biodegradable nanoparticles. Mol. Pharm. 2004; 1(1):77–84. [PubMed: 15832503]
34. Suh H, Jeong B, Rathi R, Kim SW. Regulation of smooth muscle cell proliferation using paclitaxel-loaded poly(ethylene oxide)-poly(lactide/glycolide) nanospheres. J. Biomed. Mater. Res. 1998; 42(2):331–338. [PubMed: 9773830]
35. Allen TM. Ligand-targeted therapeutics in anticancer therapy. Nat. Rev. Cancer. 2002; 2(10):750–763. [PubMed: 12360278]
36. McCarthy JR, Perez JM, Bruckner C, Weissleder R. Polymeric nanoparticle preparation that eradicates tumors. Nano. Lett. 2005; 5(12):2552–2556. [PubMed: 16351214]
37. Huff TB, Tong L, Zhao Y, Hansen MN, Cheng JX, Wei A. Hyperthermic effects of gold nanorods on tumor cells. Nanomedicine (Lond). 2007; 2(1):125–132. [PubMed: 17716198]
38. Kirui DK, Rey DA, Batt CA. Gold hybrid nanoparticles for targeted phototherapy and cancer imaging. Nanotechnology. 2010; 21(10):105105. [PubMed: 20154383]
39. Park JH, von Maltzahn G, Xu MJ, Fogal V, Kotamraju VR, Ruoslahti E, Bhatia SN, Sailor MJ. Cooperative nanomaterial system to sensitize, target, and treat tumors. Proc. Natl. Acad. Sci. U S A. 2010; 107(3):981–986. [PubMed: 20080556]
40. Collins DA, Hogenkamp HP, O'Connor MK, Naylor S, Benson LM, Hardyman TJ, Thorson LM. Biodistribution of radiolabeled adenosylcobalamin in patients diagnosed with various malignancies. Mayo. Clin. Proc. 2000; 75(6):568–580. [PubMed: 10852417]
41. Hawkins GA, McCabe RP, Kim CH, Subramanian R, Bredehorst R, McCullers GA, Vogel CW, Hanna MG Jr, Pomato N. Delivery of radionuclides to pretargeted monoclonal antibodies using dihydrofolate reductase and methotrexate in an affinity system. Cancer Res. 1993; 53(10 Suppl): 2368–2373. [PubMed: 8485723]
42. Parker N, Turk MJ, Westrick E, Lewis JD, Low PS, Leamon CP. Folate receptor expression in carcinomas and normal tissues determined by a quantitative radioligand binding assay. Anal. Biochem. 2005; 338(2):284–293. [PubMed: 15745749]
43. Smith-Jones PM, Pandit-Taskar N, Cao W, O'Donoghue J, Philips MD, Carrasquillo J, Konner JA, Old LJ, Larson SM. Preclinical radioimmunotargeting of folate receptor alpha using the monoclonal antibody conjugate DOTA-MORAb-003. Nucl. Med. Biol. 2008; 35(3):343–351. [PubMed: 18355690]
44. Zhao R, Goldman ID. Resistance to antifolates. Oncogene. 2003; 22(47):7431–7457. [PubMed: 14576850]
45. Cheng Z, Thorek DL, Tsourkas A. Gadolinium-conjugated dendrimer nanoclusters as a tumor-targeted T1 magnetic resonance imaging contrast agent. Angew. Chem. Int. Ed. Engl. 2010; 49(2): 346–350. [PubMed: 19967688]
46. Sanhai WR, Sakamoto JH, Canady R, Ferrari M. Seven challenges for nanomedicine. Nat. Nanotechnol. 2008; 3(5):242–244. [PubMed: 18654511]

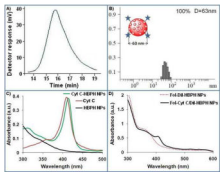

**Figure 1.**

Characterizations of the aliphatic HBPH polymer **4** and HBPH nanoparticles (HBPH NPs). A) Gel Permeation Chromatographic (GPC) trace of the polymer **4**, showing the formation of high molecular weight polymer. B) Determination of the hydrodynamic diameter of the as-synthesized HBPH nanoparticles (Cyt C-HBPH NPs) using Dynamic Light Scattering (DLS: D = 63±2 nm, PDI = 0.73). C) Comparison between the UV/Vis absorption spectrum of Cyt C encapsulating nanoparticles (Cyt C-HBPH NPs) with that of free Cyt C and HBPH nanoparticles (HBPH NPs) itself, in solution. D) UV/Vis absorbance spectra of folate functionalized DiI and Cyt C encapsulating HBPH nanoparticles.



NIH-PA Author Manuscript NIH-PA Author Manuscript NIH-PA Author Manuscript

NIH-PA Author Manuscript
NIH-PA Author Manuscript
NIH-PA Author Manuscript



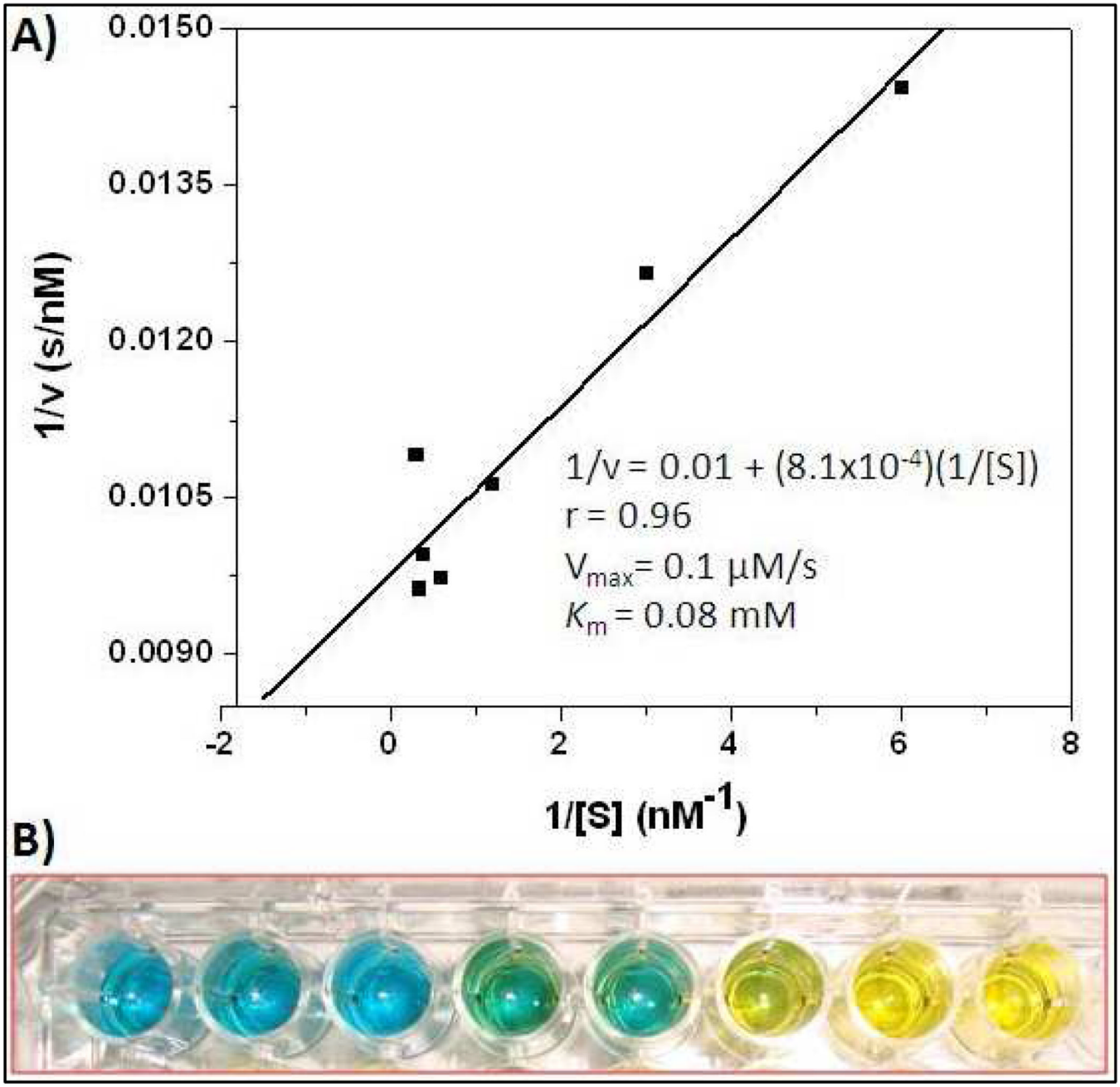


**Figure 2.**

A) Steady state kinetic assay and the double reciprocal plot of oxidase activity of Cytochrome c encapsulating HBPH nanoparticles. B) TMB assay: Retention of Cyt C-HBPH nanoparticles peroxidase activity upon encapsulation, indicating that the encapsulated Cyt C protein remained active inside the polymer matrix. Each well contains an increasing amount (from left to right, 8, 9,10,11, 12, 13, 14, 15 µL) of Cyt C HBPH nanoparticle (0.71 µg of Cyt C/mL of HBPH nanoparticle), which translate into an increasing rate of oxidation of the colorimetric TMB substrate (from blue to yellow)

NIH-PA Author Manuscript
NIH-PA Author Manuscript
NIH-PA Author Manuscript



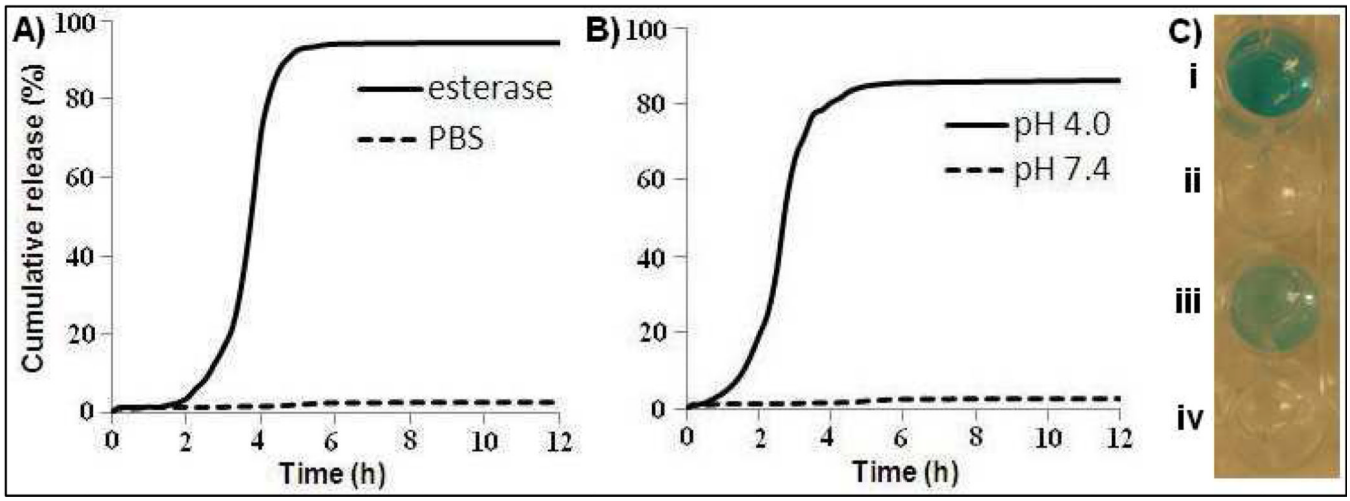


**Figure 3.**

Release profiles of Cyt C from the protein encapsulating HBPH nanoparticles (Cyt C-HBPH NPs) at 37 °C. A) A slower rate of Cyt C release was observed in the presence of an esterase enzyme, while relatively B) faster release was observed at pH 4.0. No significant release of the encapsulated Cyt C was observed in PBS (pH 7.4). C) Catalytic activity of the released Cyt C [from esterase (i) and at pH 4.0 (iii)] visualized by the oxidation of TMB with hydrogen peroxide. Absence of TMB oxidation was observed in the PBS buffer (ii, iv; pH = 7.4).

NIH-PA Author Manuscript
NIH-PA Author Manuscript
NIH-PA Author Manuscript



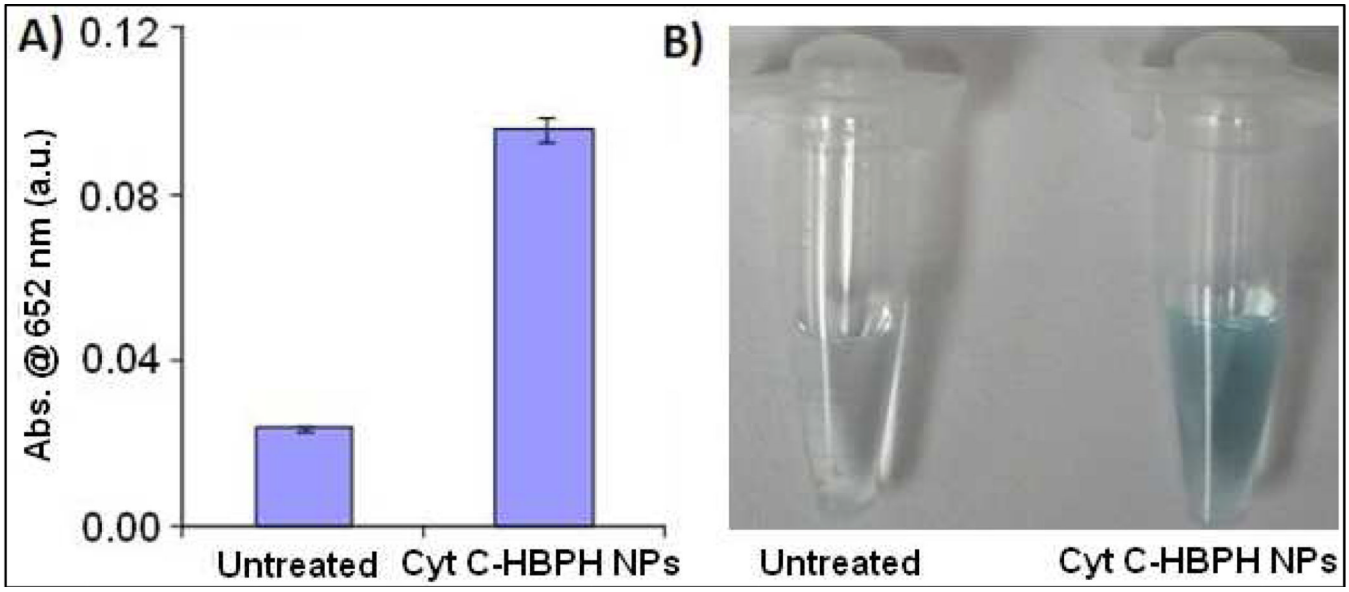


**Figure 4.**

*In vitro* retention of Cyt C-HBPH NP's cell associated peroxidase activity. A) MCF 7 cells treated (6 h) with Cyt C-HBPH nanoparticle displayed peroxidase activity when the cell pellet was dissolved in TMB solution, indicated that the protein was still active upon release within the cell. B) images showing the blue color of the oxidized TMB solution compared to untreated.

NIH-PA Author Manuscript
NIH-PA Author Manuscript
NIH-PA Author Manuscript



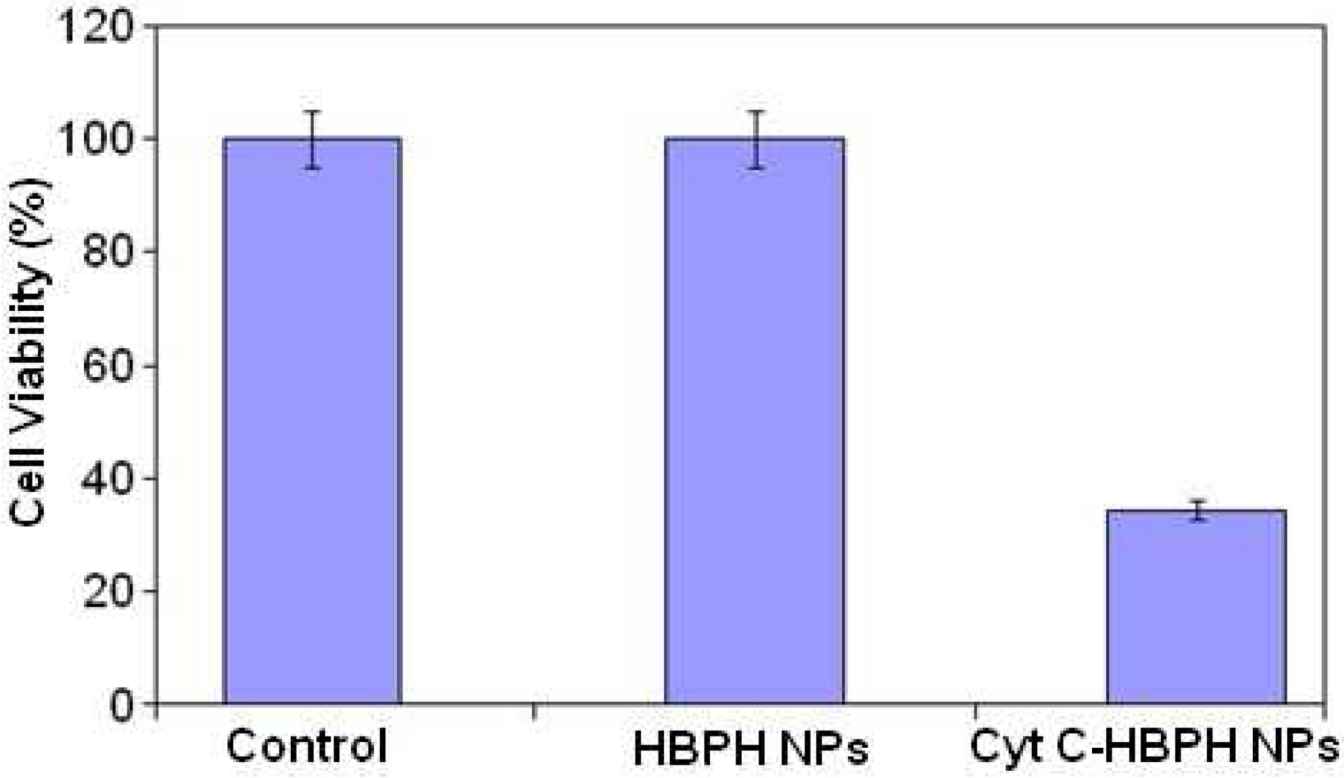


**Figure 5.**

Cell viability of MCF 7 cells treated with Cyt C encapsulating HBPH nanoparticles (Cyt C-HBPH NPs) compared to that of cells treated with the non-encapsulated nanoparticle (HBPH NPs) and non-treated cells (control). The protein encapsulating HBPH nanoparticles induced a significant reduction in the cell (MCF 7) viability after 6 h of incubation, where the non-encapsulated nanoparticle (HBPH NPs) showed no significant cytotoxicity. Control cells (MCF 7) were treated with 1× PBS. Average values of four measurements were depicted ± standard error.

NIH-PA Author Manuscript
NIH-PA Author Manuscript
NIH-PA Author Manuscript



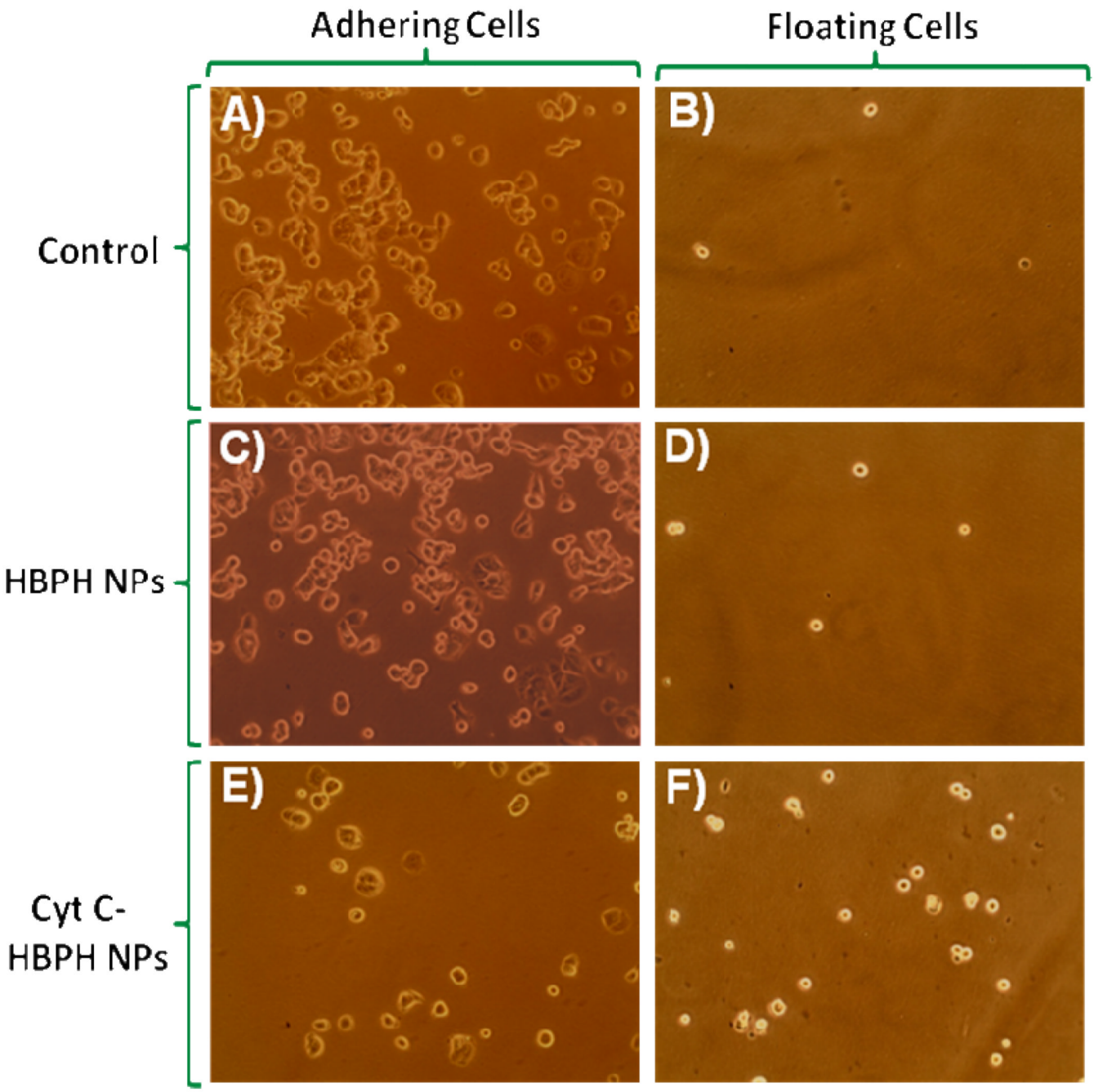


**Figure 6.**
MCF 7 cells showing the cytotoxic effect of the Cyt C encapsulating HBPH nanoparticles. Cells incubated with non-encapsulated nanoparticles (HBPH NPs) showed no cell death (C and D) similar to control cells (A and B). Cyt C encapsulating HBPH nanoparticles (Cyt C-HBPH NPs) induced significant cellular death as very less number of cells was found adhering to the plate (E) and an increase number of cell were found floated (F).

NIH-PA Author Manuscript
NIH-PA Author Manuscript
NIH-PA Author Manuscript



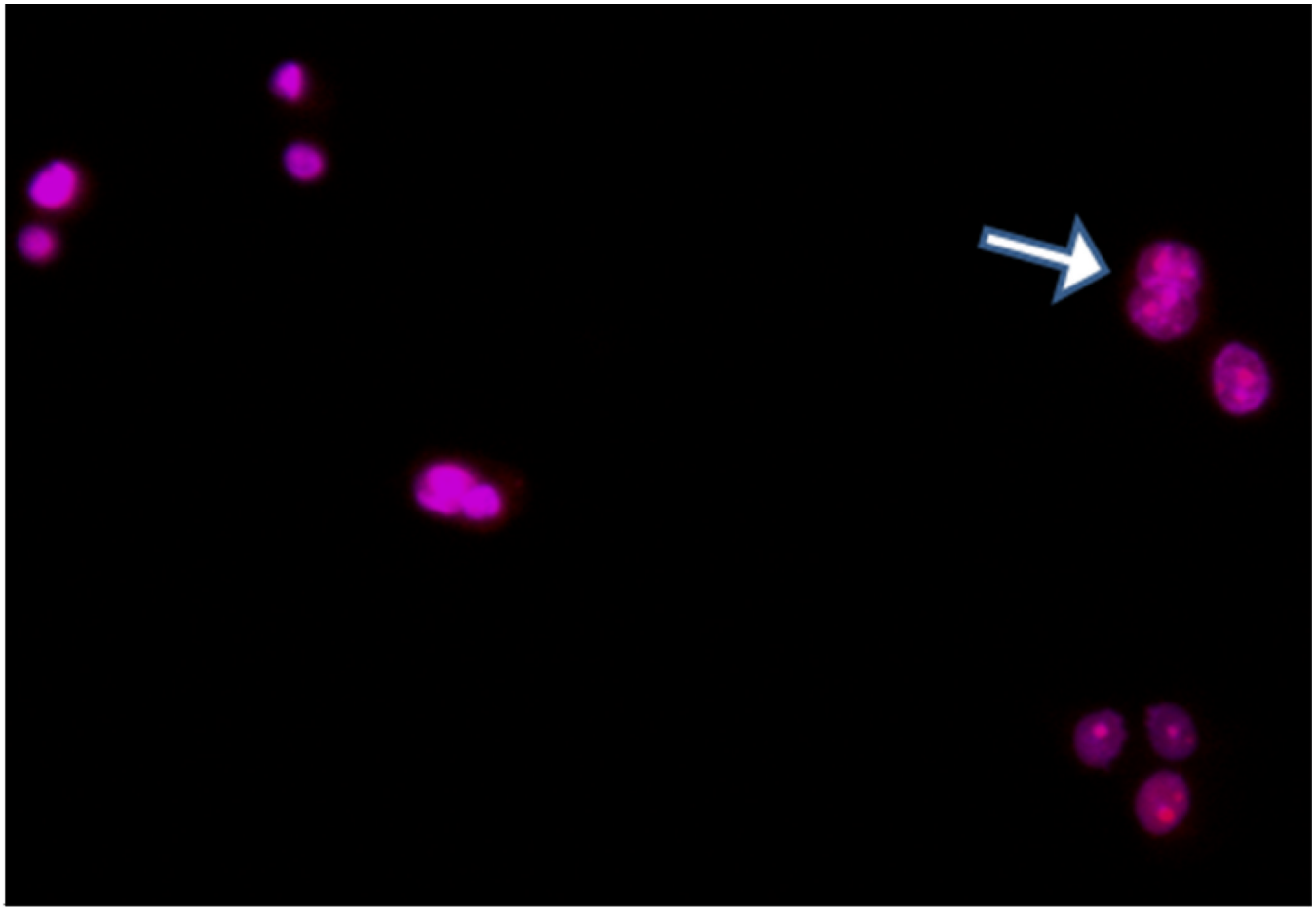

**Figure 7.**
Detection of apoptotic cells. Induction of apoptosis observed when MCF 7 cells were treated with Cyt C encapsulating HBPH nanoparticles (Cyt C-HBPH NPs) and stained with DAPI and propidium iodide (PI) after 6 h of incubation. The arrow showed nuclear fragmentation indicating apoptosis.

NIH-PA Author Manuscript
NIH-PA Author Manuscript
NIH-PA Author Manuscript



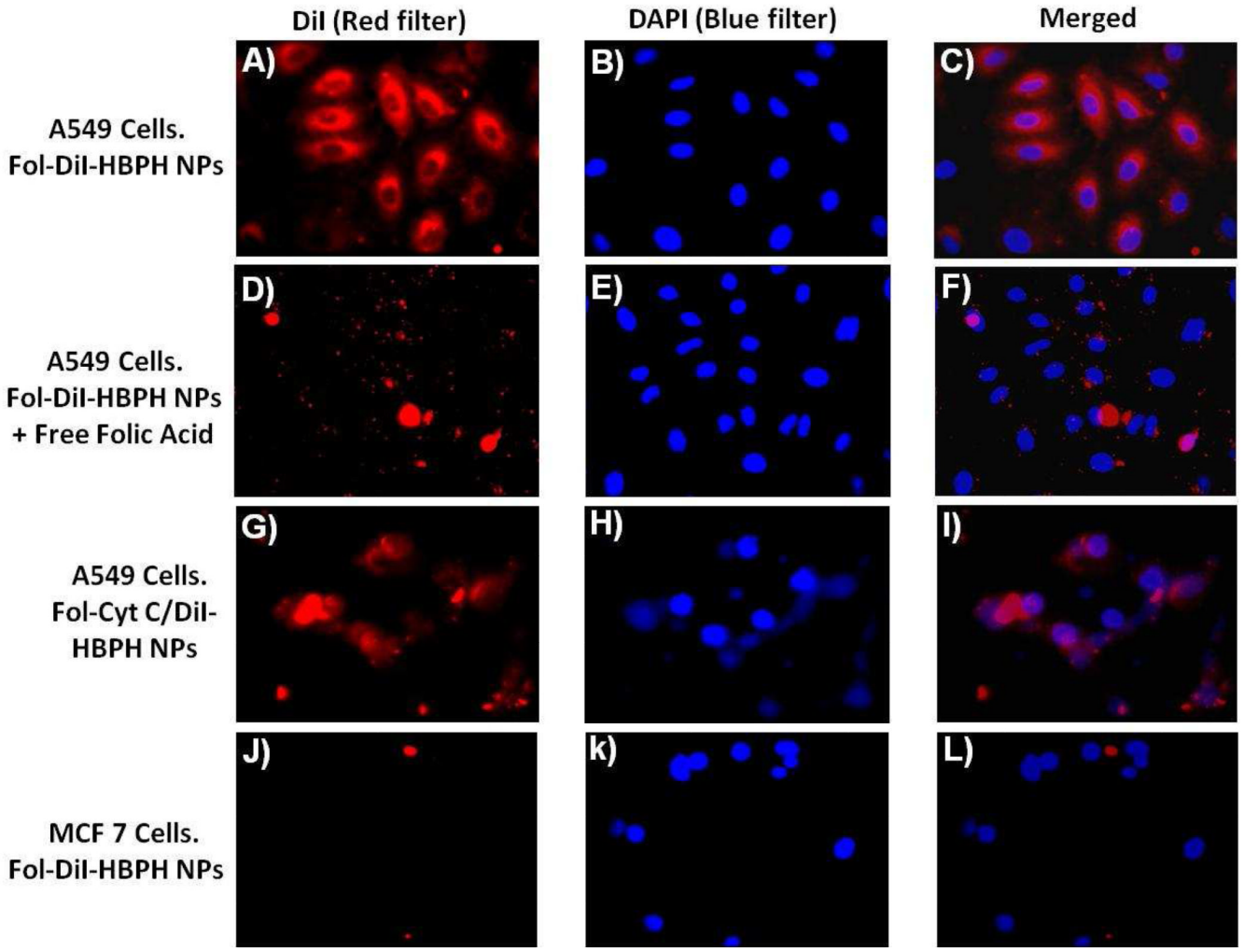


**Figure 8.**

Assessment of folate-HBPH nanoparticle uptake by human lung carcinoma A549 cells (A–I) and human breast adenocarcinoma MCF 7 cells (J–L) via confocal laser-scanning microscopy. Enhanced cellular internalization was observed upon incubation of the folate conjugated DiI-encapsulating HBPH nanoparticles (Fol-DiI-HBPH NPs) with A549 cells (A–C). In contrast, A549 cells pre-incubated with free folic acid showed minimal uptake (D–F), confirming receptor-mediated internalization. Meanwhile, A549 cells incubated with the Cyt C and DiI co-encapsulating folate-functionalized HBPH nanoparticles (Fol-Cyt C/DiI-HBPH NPs) induced significant cell death (G–I). As expected, no internalization of the Fol-DiI-HBPH NPs was observed in the MCF 7 as these cells are folate-receptor negative (J–L).

NIH-PA Author Manuscript

NIH-PA Author Manuscript

NIH-PA Author Manuscript

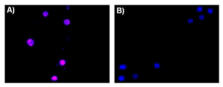


**Figure 9.**

Detection of apoptotic cells. A) Selective induction of apoptosis observed in A549 cells (folate-receptor positive) and B) no cellular apoptosis observed in MCF 7 cells (folate-receptor negative) when incubated with folate conjugated Cyt C encapsulating HBPH nanoparticles (Fol-Cyt C-HBPH NPs), stained with DAPI and propidium iodide (PI) after 6 h of incubation.

NIH-PA Author Manuscript
NIH-PA Author Manuscript
NIH-PA Author Manuscript



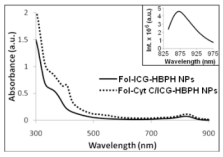


**Figure 10.**

UV-Vis absorbance spectra of the folate conjugated HBPH nanoparticles encapsulated with ICG (Fol-ICG-HBPH NPs) and Cyt C (Fol-Cyt C/ICG-HBPH NPs), showing absorbance at 355 nm, 414 nm and at 835 nm for folic acid, encapsulated Cyt C and ICG dye, respectively. Inset: Fluorescence emission spectra of the Fol-ICG-HBPH nanoparticles showing emission maximum at 865 nm. Similar results obtained from the corresponding Cyt C encapsulating HBPH nanoparticles.

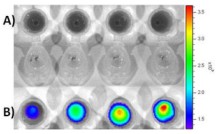


**Figure 11.**

Near infrared fluorescence images of the ICG encapsulating HBPH nanoparticles (Fol-ICG-HBPH NPs) incubated with A) MCF 7 and B) A549 cells, indicating receptor-mediated internalizations of our theranostic HBPH nanoparticles. Images taken from a Xenogen IVIS system using ICG filter set. Each well contains an increasing amount (from left to right, 20, 40, 60 80 μL) of Fol-ICG-HBPH NPs (3.2 mg/mL), which translate into an increasing uptake of nanoparticles and higher fluorescence emission.

NIH-PA Author Manuscript
NIH-PA Author Manuscript
NIH-PA Author Manuscript

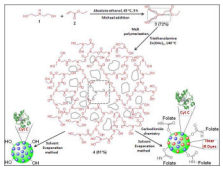

**Scheme 1.**

Schematic representation of the synthesis of three dimensional hydrophilic HBPH polymer (**4**) and its functional HBPH nanoparticles (HBPH NPs). The monomer **3** with three-bond connectivity polymerized three-dimensionally, resulting in a highly branched polymer with amphiphilic cavities in the polymeric structure.

NIH-PA Author Manuscript
NIH-PA Author Manuscript
NIH-PA Author Manuscript